FULL PAPER

Dalton
www.rsc.org/dalton

Oxovanadium(IV) complexes of salicyl-L-aspartic acid and salicylglycyl-L-aspartic acid†

Tamás Jakusch,[a] Susana Marcão,[b] Lígia Rodrigues,[c] Isabel Correia,[b] João Costa Pessoa*[b] and Tamás Kiss*[a,d]

[a] *Bioinorganic Chemistry Research Group of the Hungarian Academy of Sciences, Department of Inorganic and Analytical Chemistry, University of Szeged, POBox 440, H-6701 Szeged, Hungary*

[b] *Centro Química Estrutural, Instituto Superior Técnico, Av. Rovisco Pais, 1049-001 Lisboa, Portugal*

[c] *Departamento de Química, Universidade do Minho, Largo do Paço, 4709 Braga, Portugal*

[d] *Department of Inorganic and Analytical Chemistry, University of Szeged, POBox 440, H-6701 Szeged, Hungary*

Received 12th May 2005, Accepted 15th July 2005
First published as an Advance Article on the web 11th August 2005

The dipeptide and tripeptide analogues salicyl-L-aspartic acid (Sal-L-Asp) and salicylglycyl-L-aspartic acid (SalGly-L-Asp) were synthesized and their protonation and complex formation with $V^{IV}O^{2+}$ were studied in aqueous solution through the use of pH-potentiometry and spectroscopic (UV-Vis, CD and EPR) techniques. The phenolate terminus proved to be a good anchoring site to promote (i) the metal ion-induced deprotonation and subsequent coordination of the peptide amide group(s) in the pH range 4–5 for the dipeptide analogue, (ii) and in the pH range 5–6 in a very cooperative way for the tripeptide analogue. The results suggest that the presence of good anchoring donors on both sides of the amide groups is responsible for the cooperative deprotonation of the two amide-NH groups.

Introduction

The metal binding ability of a simple oligopeptide is strongly determined by the presence in the ligand molecule of a suitable anchoring donor, which can bind metal ions strongly enough to promote deprotonation of the amide-NH. Various metal ions have been found to be able to do this, *e.g.* Pt(II), Pd(II), Cu(II), Ni(II), and in some special cases Zn(II), Co(II), and certain others.[1] This results in an (anchoring donor, CON^-, $COO^-)_{eq}$ binding mode [below we represent phenolate-O^-, and amide-N^- by O^- and CON^-, respectively, while $(X,Y,\ldots)_{eq}$ and $(X)_{ax}$, mean that the donor atoms X, Y,... are coordinated in the equatorial or the axial position, respectively], corresponding to a strong interaction between the metal ion and the oligopeptide. These basic binding modes may be modified considerably by strongly coordinating side-chain donors, such as imidazole-N or thiolate-S.

With $V^{IV}O^{2+}$, neither the terminal NH_2 nor the terminal COO^- is a sufficiently strong binder to behave as an efficient anchoring donor in the promotion of amide deprotonation.[2] However, phenolate is known to have a much higher affinity for $V^{IV}O^{2+}$. Accordingly, replacement of the terminal NH_2 group by the phenolate-O^- enhances the metal-binding ability of the molecule significantly. In fact, both the dipeptide analogue 2-OH-hippuric acid (salicylglycine, SalGly) and the tripeptide analogue SalGly-L-Ala (for their formulae, see Scheme 1) proved to be strong $V^{IV}O^{2+}$ binders: they keep $V^{IV}O^{2+}$ in solution in the pH range 2–12, even in equimolar ratio. No precipitation or slow equilibration indicative of hydrolysis of the metal ion or its complexes is observed in these systems. Detailed pH-metric and spectral studies[3,4] have indicated that strong coordination of the ligands to $V^{IV}O^{2+}$ can induce deprotonation of the peptide-NH group(s), and the complexes containing the binding mode $(O^-, CON^-, COO^-, H_2O)_{eq}$ for SalGly, and $(O^-,CON^-,CON^-,COO^-)_{eq}$ for SalGly-L-Ala, become the predominant species by pH ~ 6.

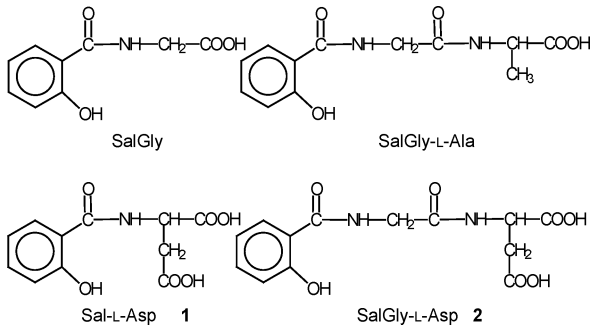

Scheme 1

Interestingly, deprotonation of the two adjacent amide-NH groups in VO(SalGly-L-Ala) takes place in a strongly overlapping way (pK(VOL) = 5.37 and pK(VOLH$_{-1}$) = 5.39); the intermediate species containing one deprotonated amide-N^- group being formed only in low concentration. Amide coordination is accompanied by a characteristic colour change from blue to pinkish-red at pH ~ 5.5, with hardly any subsequent change up to pH ~ 11. The changes in the EPR parameters indicate more covalent bonding in the equatorial plane, which is in accordance with the above-mentioned rearrangement of the binding modes. A detailed analysis of the CD data (including deconvolution of the data for the individual species) on the $V^{IV}O$–SalGly-L-Ala system revealed that a strong CD signal accompanies only the formation of $[VOLH_{-2}]^{2-}$, with both peptide-N^- atoms equatorially coordinated. This indicates that, although the deprotonation of the two amides take place in a cooperative way, it starts on the one closer to the phenolate terminal. This is in agreement with what has been observed for most metal ions, but is in contrast with what was found for R_2Sn(IV), where the C-terminal COO^- proved to be the anchoring donor.[5]

In the presence of an extra carboxylate in Asp-containing dipeptides, the $V^{IV}O^{2+}$-binding ability of the ligands is somewhat increased as compared with that of the Gly-type dipeptides,

† Electronic supplementary information (ESI) available: Fig. SI-1–SI-5. See http://dx.doi.org/10.1039/b506684k

DOI: 10.1039/b506684k

because of the presence of new chelating sites: (COO^-, COO^-) in GlyAsp and (NH_2, COO^-) in AspGly. Although these sites are more efficient for $V^{IV}O^{2+}$ binding, the extent of amide deprotonation/coordination is hardly enhanced as compared with the Gly-type dipeptides.[6]

In this work the pseudo di- and tri-peptides analogues of salicylic acid, containing aspartic acid in the C terminal position: Sal-L-Asp **1** (L^1) and SalGly-L-Asp **2** (L^2) were synthesized and their $V^{IV}O^{2+}$-binding abilities were studied by means of pH-potentiometric and spectroscopic techniques.

Experimental

Preparation of Sal-L-Asp 1

Synthesis of L-Asp(OMe)OMe. Thionyl chloride (25 ml) was added dropwise to stirred and cooled (−10 °C) methanol (100 ml), followed by the addition of L-Asp (6.66 g, 50 mmol). The temperature of the solution was then increased to 40 °C for 2 h. The solvent was removed next and the oil obtained, after crystallization from methanol–diethyl ether, afforded the pure compound (7.8 g, 79%, mp 115–116 °C).

NMR-DMSO$_{d6}$ 3.00–3.03 (2H, m, CH_2); 3.74 and 3.64 (6H, 2s, 2 × OCH_3); 4.32 (1H, t *J* 5.7 Hz, CH); 8.79 (3H, br s, NH_3^+).

Sal-L-Asp(OMe)OMe. Salicylic acid (2.76 g, 20 mmol) was dissolved in ethyl acetate (80 ml) and the solution was cooled to 0 °C. Dicyclohexylcarbodiimide (DCC) (4.3 g, 21 mmol), L-Asp(OMe)OMe (3.95 g, 20 mmol) and triethylamine (3.6 ml, 20 mmol) were added successively. The reaction mixture was stirred overnight at room temperature. The insolubles were then filtered off and the solution was washed in turn with 5% citric acid, water, 5% $NaHCO_3$ and water. After drying over $MgSO_4$, the solution was concentrated. The residue was taken up in a minimum amount of acetone and left at ~0 °C for 4 h. The precipitated solid was filtered off and the solution was concentrated. The oil obtained proved resistant to crystallization (4.48 g, 79%).

NMR-DMSO$_{d6}$ 2.90–3.20 (2H, m, CH_2Asp); 3.69–3.78 (1H, m, αCHAsp); 6.91 (2H, apparent t *J* 7.8 Hz); 7.40 (1H, apparent t *J* 8.0 Hz) 7.86 (1H, dd *J* 1.2 and 8.0 Hz,); 8.90 (1H, d *J* 8.1 Hz, NHAsp); 12.40 (1H, br s, OH).

Sal-L-Asp 1. Sal-L-Asp(OMe)OMe (4.47 g, 15.9 mmol) was dissolved in methanol (30 ml) and 1 M NaOH (50 ml, 50 mmol) was added. The mixture was stirred at room temperature for 2 h, and 1 M HCl (16 ml, 16 mmol) was added. The methanol was removed at reduced pressure and the solution thus obtained was cooled in an ice bath and acidified with 1 M HCl (34 ml) under vigorous stirring. The white solid that precipitated out was filtered off, washed with water and dried (1.2 g, 30%, mp 171–172 °C).

NMR-DMSO$_{d6}$ 2.84–2.81(2H, m, βCH2Asp); 4.75 (1H, apparent q *J* 8.1 Hz, αCHAsp), 6.91 (2H, apparent t *J* 7.2 Hz); 7.39 (1H, td *J* 1.8 and 8.0 Hz), 7.88 (1H, dd *J* 1.8 and 8.2 Hz); 9.13 (1H, d *J* 8.1 Hz, NH); 12.85 (1H, s, OH); 12.60 (2H, br s, OH).

Found: C, 52.4; H, 4.6; N, 5.5. Calcd. for $C_{11}H_{11}O_6N$: C, 52.18; H, 4.65; N, 5.18%.

Preparation of SalGly-L-Asp 2

Boc·Gly-L-Asp(OMe)OMe. This was prepared by the DCC method on a 10 mmol scale. The chromatographically pure oil obtained (2.75 g, 86%) resisted crystallization.

NMR-DMSO$_{d6}$ 1.36 (9H, s, Boc); 2.72–2.77 (2H, m, CH_2Asp); 3.50 (2H, d *J* 6 Hz, CH_2Gly); 3.61 and 3.59 (3 + 3H, s, 2 × OCH_3); 4.66 (1H, apq *J* 7.8 Hz, αCHAsp); 6.97 (1H, t *J* 6 Hz, NHGly); 8.23 (1H, d *J* 8 Hz, NH-Asp).

TFA·Gly-L-Asp(OMe)OMe. The protected peptide Boc·Gly-L-Asp(OMe)OMe (5 mmol, 1.598 g) was treated with trifluoroacetic acid (TFA) (25 ml) and left at room temperature, protected from moisture, with occasional stirring for 1 h. The solution was then concentrated and diethyl ether was added. The mixture was cooled. The ether was decanted off and the oil obtained was dried. A solid foam was obtained in quantitative yield and used in the next step without further purification.

NMR-DMSO$_{d6}$ 2.78–2.82 (2H, m, αCH_2Asp); 3.63 (3H, s, OCH_3); 3.61 (5H, s + overlapped, CH_2Gly + OCH_3); 4.71 (1H, apq *J* 7.2 Hz, αCHAsp); 8.09 (3H, br s, NH_3^+); 8.95 (1H, d *J* 8 Hz, NH-Asp).

SalGly-L-Asp(OMe)OMe. Salicylic acid (0.69 g, 5 mmol) was dissolved in ethyl acetate (20 ml) and the solution was cooled to 0 °C. DCC (1.08 g, 5.2 mmol), compound TFA·Gly-L-Asp(OMe)OMe (1.66 g, 5 mmol) and triethylamine (0.9 ml, 5 mmol) were added successively. The reaction mixture was stirred overnight at room temperature. The insolubles were filtered off and the solvents were removed under reduced pressure. The residue was taken up in a minimum amount of acetone and left at 0 °C for 4 h. The precipitated solid was filtered off (DCHU) and the solution was concentrated. The oil obtained resisted crystallization (1.091 g, 67%).

NMR-DMSO$_{d6}$ 2.70 and 2.80 (2H, dd *J* 1.5 and 6.0 Hz, αCH_2Asp); 3.60 and 3.62 (6H, 2s, 2 × OCH_3); 3.94 (2H, d J 5.4 Hz, CH_2Gly); 4.70 (1H, apq *J* 6.0 Hz, αCHAsp); 6.90–6.92 (2H, m, 3-H and 5-H); 7.39 (1H, tap *J* 8.1 Hz, 4-H) 7.86 (1H, dd *J* 0.9 and 8.4 Hz, 6-H); 8.54 (1H, d *J* 8.1 Hz, NHAsp); 9.08 (1H, t *J* 6.0 Hz, NHGly); 12.20 (1H, s, Ar-OH).

SalGly-L-Asp. SalGly-L-Asp(OMe)OMe (1.090 g, 3.22 mmol) was dissolved in methanol (10 ml) and an aqueous solution of 1 M NaOH was added (9.69 ml). The mixture was stirred at room temperature for 4 h, and 1 M HCl (3.3 ml) was then added. The methanol was removed under reduced pressure and the solution obtained was cooled in an ice-bath and acidified with 1 M HCl (6.4 ml) under vigorous stirring. This aqueous solution was extracted three times with ethyl acetate; the organic layers were collected, dried over magnesium sulfate and filtered and the solvent was removed. A solid foam was obtained (585 mg, 58%). An attempt of crystallization from a mixture of methanol, diethyl ether and petroleum spirit afforded a white solid, melting at 105–107 °C.

NMR-DMSO$_{d6}$ 2.60 and 2.70 (2H, dd J 1.5 and 6.0 Hz, βCH_2Asp); 3.94 (2H, d J 5.7 Hz, CH_2Gly); 4.56 (1H, apq *J* 6.0 Hz, αCHAsp); 6.86–6.92 (2H, m, 3-H and 5-H); 7.39 (1H, tap *J* 8.1 Hz, 4-H) 7.86 (1H, dd *J* 0.9 and 8.4 Hz, 6-H); 8.37 (1H, d *J* 7.8 Hz, NHAsp); 9.06 (1H, t *J* 5.7 Hz, NHGly); 12.20 (1H, s, Ar–OH): 12.60 (2H, br s, CO_2H).

Anal. Calcd. for $C_{14}H_{18}N_2O_5 + 1/2\ C_4H_8O_2$ (ethyl acetate): C 50.85, H 5.08, N 7.91. Found: C 50.2, H 5.4, N 7.9.

pH-Potentiometric measurements

The protonation constants of Sal-L-Asp and SalGly-L-Asp and the stability constants of their $V^{IV}O^{2+}$ complexes were determined at 25 °C by pH-metric titration of 10 cm^3 samples. The pHs were measured with an Orion 720A pH-meter equipped with an Metrohm 6.0234.100 combined glass electrode calibrated for hydrogen ion concentration.[7] The ligand concentrations were 0.0020 and 0.0040 mol dm^{-3} and the ligand to metal molar ratios were 4 : 4, 4 : 2, 4 : 1, 2 : 2 and 2 : 1. Titrations were performed with KOH solution of known concentration (*ca.* 0.2 mol dm^{-3}) under a purified argon atmosphere, to avoid interference from oxygen and carbon dioxide in the air. The pH range studied was normally from 2 to 10 unless extensive hydrolysis or a very slow equilibrium was detected. The reproducibility of titration points included in the evaluation was within 0.005 pH units in the whole pH range. A pK_w value of 13.76 was determined and used for the titrations at 25 °C and I = 0.20 mol dm^{-3} KCl.

The concentration stability constants $\beta_{pqr} = [M_pL_qH_r]/[M]^p[L]^q[H]^r$ were calculated using the PSEQUAD computer program.[8] The formation of the hydroxo complexes of $V^{IV}O^{2+}$ was taken into account. The following species were assumed: $[V^{IV}O(OH)]^+$ ($\log \beta_{10-1} = -5.94$), $[(V^{IV}O)_2(OH)_2]^{2+}$ ($\log \beta_{20-2} = -6.95$), with stability constants calculated from the data of Henry *et al.*[9] and corrected for the different ionic strength by using the Davies equation. $[(V^{IV}O)_2(OH)_5]^-$ ($\log \beta_{20-5} = -22.5$) and $[V^{IV}O(OH)_3]^-$ ($\log \beta_{10-3} = -18.0$) were also included.[10,11]

Instrumentation and procedures

Physical measurements on the ligands. Melting points were determined on a Gallenkamp melting point apparatus and are uncorrected. NMR data were recorded on a Varian Unity Plus 300 Spectrometer in the solvent indicated. Elemental analyses were carried out on a Leco CHNS 932 instrument.

Spectroscopic measurements. The CD spectra were recorded with a JASCO 720 spectropolarimeter with a red-sensitive photomultiplier (EXEL-308), and visible spectra with a HITACHI U2000 or a OOIChem S2000/PC2000 (the spectral range covered was normally-Vis-400–900 or 370–880, and in the case of CD 400–1000 nm). The EPR spectra were recorded at 77 K with a Bruker ESR-ER 200D X-band spectrometer. The EPR parameters were obtained by simulation of the spectra with the computer program of Rockenbauer and Korecz.[12]

CD, Vis and EPR spectra of $V^{IV}O^{2+}$–Sal-L-Asp system (I) and $V^{IV}O^{2+}$–SalGly-L-Asp system (II) systems were recorded by varying the pH at approximately fixed total vanadium and ligand concentrations. For system I, the L^1 : M ratio was 2.6 (with $C_{VO} \sim 0.003$ mol dm^{-3}). For system II the L^2 : M ratios used were as follows: 1.4 for IIa, 2.7 for IIb, and 1.2 for IIc ($C_{VO} \sim 3$ mol dm^{-3} in IIa and IIb, and $C_{VO} \sim 5.5$ mol dm^{-3} in IIc). Unless otherwise stated, by visible (Vis) spectra and CD spectra we mean representations of either ε_m or $\Delta\varepsilon_m$ values *versus* λ [ε_m = absorption/(bC_M), and $\Delta\varepsilon_m$ = (differential absorption)/(bC_M) where b = optical pathlength and C_M = total metal concentration].

Results and discussion

Sal-L-Asp **1** and SalGly-L-Asp **2** were synthesized by the procedures described in the Experimental. Their formulae are depicted in Scheme 1. The protonation and $V^{IV}O$ complex formation constants of the ligands are listed in Table 1. Both ligands contain three dissociable protons: on the phenolic OH group and the two terminal COOH groups. The protonation constants (log K values) of 2.93 and 4.50 for **1** and of 2.90 and 4.49 for **2** can be assigned to the COOH functions present in the peptides, while the log K_{OH} values of 8.38 for **1** and 7.94 for **2** in the basic pH range are assigned to the phenolic OH groups. The concentration distribution curves of the complexes formed in $V^{IV}O$-Sal-L-Asp and $V^{IV}O$-SalGly-L-Asp systems are shown in Fig. 1.

Table 1 Protonation (log K) and $V^{IV}O$ complex formation constants (log β with 3 S.D. values in parentheses) of the ligands studied at t = 25 °C and I = 0.2 mol dm^{-3} (KCl)

Species	Sal-L-Asp	SalGly-L-Asp
log K_1	2.93(2)	2.90(2)
log K_2	4.50(1)	4.49(1)
log K_3	8.38(1)	7.94(1)
$VOL^{1,2}H_2$	15.09(8)	14,1(2)
$VOL^{1,2}H$	11.88(3)	11.10(6)
$VOL^{1,2}$	7.88(3)	7.46(3)
$VOL^{1,2}H_{-1}$	3.09(2)	~0.9[b]
$VOL^{1,2}H_{-2}$	−5.00(5)	−4.53(10)[c]
pK($VOL^{1,2}H_2$)	3.21	3.0
pK($VOL^{1,2}H$)	4.00	3.54
pK($VOL^{1,2}$)	4.79	~6.5
pK($VOL^{1,2}H_{-1}$)	8.09	~5.5
No. of points	345	348
Fitting[a] (Δcm^3)	2.37 × 10^{-3}	5.95 × 10^{-3}

[a] Average difference between the experimental and calculated titration curves expressed in the volume of the titrant. [b] Estimation from the Vis and the LN EPR spectra [c] Average value, calculated from pH-metry, Vis-, CD-, LN and RT EPR spectra.

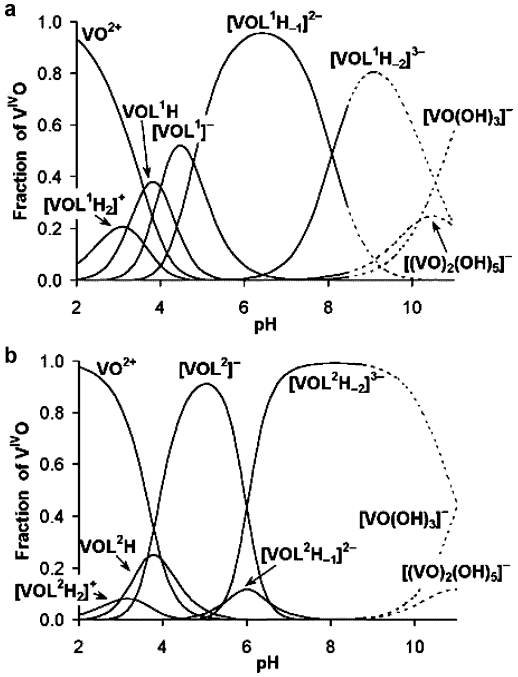

Fig. 1 Concentration distribution curves of complexes formed in solutions containing (a) $V^{IV}O^{2+}$ and Sal-L-Asp, with $C_{VO} = 0.001$ mol dm^{-3} and L : M = 4, and (b) $V^{IV}O^{2+}$ and SalGly-L-Asp with $C_{VO} = 1$ mM and L : M = 4, calculated by using the stability constants listed in Table 1.

It is noteworthy that there is some uncertainty in the calculation of $\beta(VOL^2H_{-1})$ of system II from pH-metric data. Change of the value of log $\beta(VOL^2H_{-1})$ from 0 to 1.5 has almost no effect on the fitting parameter and the other log β values. Several calculations for log $\beta(VOL^2H_{-1})$ and log $\beta(VOL^2H_{-2})$ based on the Vis, CD and EPR spectra (see ESI†) resulted in log $\beta(VOL^2H_{-1}) \sim 0.9$ and log $\beta(VOL^2H_{-2}) = -4.53 \pm 0.10$. As discussed below, the spectroscopic data indicate the formation of only a small amount of $[VOL^2H_{-1}]^{2-}$ (maximum ~10%), therefore the formation constants obtained from the spectroscopic data were accepted. pH-metry has a tendency to overestimate the extent of formation of the species $[VOL^2H_{-1}]^{2-}$; this is possibly due to the uncertainty in the log $\beta[(VO)_2(OH)_5]^-$ value, which appears in low concentration in the same pH range.

Sal-L-Asp system

The Vis spectra recorded for this system at different pH values are depicted in Fig. S1 of ESI†. At very low pH, the spectra resemble that of $[VO(H_2O)_5]^{2+}$. In agreement with the speciation curves, the visible spectra start to deviate from that of the aqua ion at pH > 2, where the formation of the protonated species $[VOL^1H_2]^+$ and $[VOL^1H]$ are indicated by the speciation curves. The spectral intensity in the near UV region (350–400 nm) starts to increase at lower pH than for the formation of the $[VOL^1]^-$ suggesting that the deprotonated phenolate oxygen takes part of the coordination in both species $[VOL^1H]$ and $[VOL^1H_2]^+$. In Scheme 2, some of the most probable isomeric binding modes are presented for $[VOL^1H_2]^+$: (O^-, O_{amide}, 2 × $H_2O)_{eq}$, (COO^-, O_{amide}, 2 × $H_2O)_{eq}$ and for $[VOL^1H]$: (COO^-, O_{amide}, O^-, $H_2O)_{eq}$, (2 × COO^-, 2 × $H_2O)_{eq}$.

As the pH is increased (up to pH 7.5) there is a small shift of the λ_{max} to higher wavelengths. Between pH 5 and 8, a new band

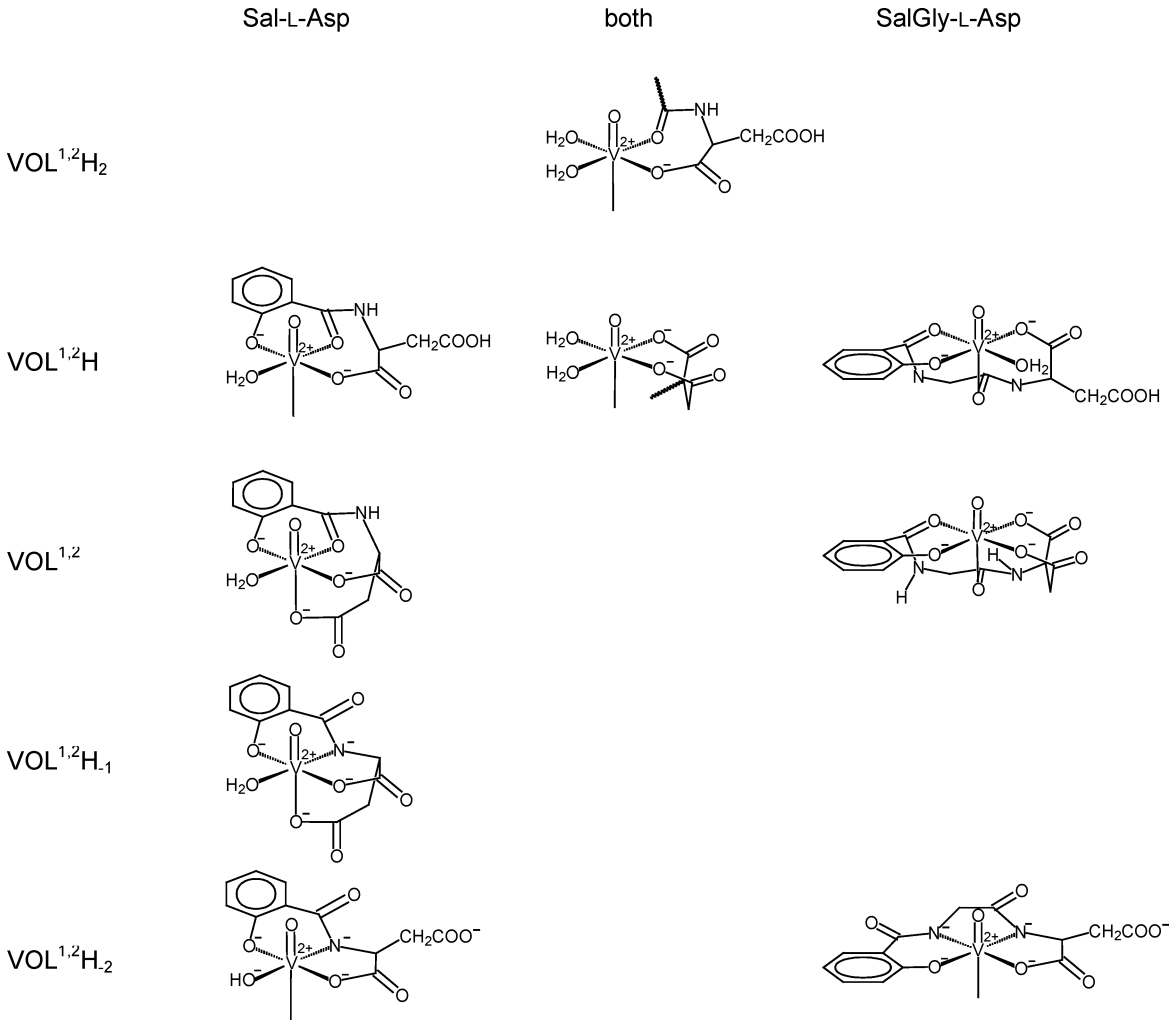

Scheme 2

is observed at $\lambda_{max} \sim 510$ nm. At pH > 9, binary and ternary OH^- containing species are formed.

The CD spectra for system I (Fig. 2) are in good agreement with the species distribution (Fig. 1). Starting from pH ~ 3.0, in parallel with the formation of $[VOL^1]^-$, the intensity of the CD spectra (a negative band at around $\lambda = 790$–800 nm) increases up to the maximum amount of $[VOL^1H_{-1}]^{2-}$. As $[VOL^1]^-$ starts to deprotonate (pH ~ 4), a new negative band appears at ~ 490 nm. At pH ~ 6.3, the CD shows maximum intensity, with two negative bands at ~790 nm and ~490 nm ($\Delta\varepsilon = -0.6$ and -0.35 mol^{-1} dm^{-3} cm^{-1}, respectively), which can be assigned to the formation of $[VOL^1H_{-1}]^{2-}$. The pattern of the spectrum is similar to that for $V^{IV}O$–*N*-acetyl aspartic acid system,[6] suggesting its related to the coordination of two carboxylate groups. At higher pH values the intensity decreases, and for pH > ~ 8.5 the pattern of the CD spectra changes, indicating the formation of a different species, a ternary hydroxo complex with $[VOL^1H_{-2}]^{3-}$ stoichiometry. As the shape of the spectra differs from what was measured in the system $V^{IV}O$–*N*-acetyl aspartic acid,[6] we assume that the side-chain carboxylate group of Asp was already displaced from the coordination sphere of the metal ion, probably because of the increased charge of the species.

The experimental visible and CD spectra obtained at different pH values were used to calculate the spectra of each individual species for the $V^{IV}O$-Sal-L-Asp system, using the PSEQUAD computer program. Good CD and visible spectra could be simulated for each species (see Fig. 3). This confirms the validity of the speciation model proposed and the reliability of the stability constants calculated from pH-metric studies and the spectroscopic data obtained from the spectral measurements.

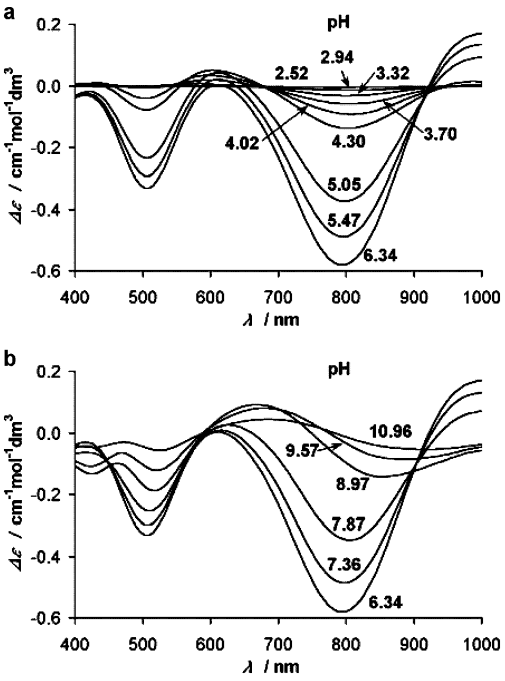

Fig. 2 CD spectra of solutions containing $V^{IV}O^{2+}$ (0.003 mol dm^{-3}) and Sal-L-Asp (0.008 mol dm^{-3}) at different pH values in the range: 2.52–6.34 (a) and 6.34–10.96 (b).

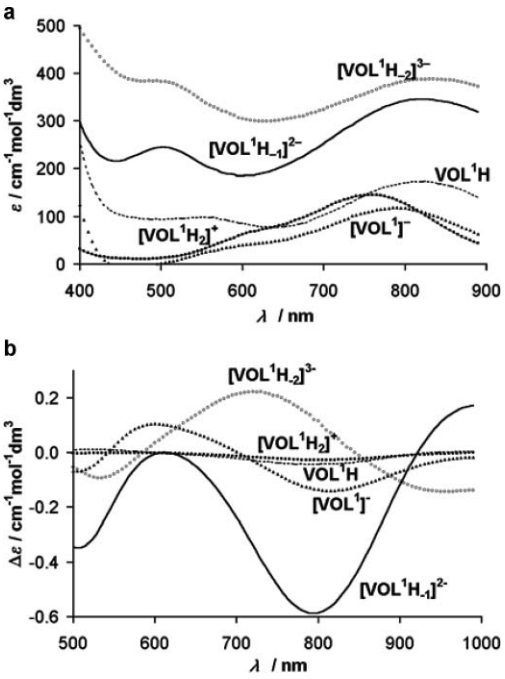

Fig. 3 Calculated Vis spectra of each individual species formed in the $V^{IV}O$-Sal-L-Asp system, using the program PSEQUAD and the formation constants listed in Table 1.

SalGly-L-Asp system

Up to pH 4.9 the spectra recorded for the two systems are similar in type and resemble those for the $V^{IV}O^{2+}$–*N*-acetyl-L-aspartic acid system.[6] One main negative band is observed at $\lambda \sim 750$ nm ($\Delta\varepsilon = -0.25$ mol^{-1} dm^{-3} cm^{-1}), with a shoulder at ~650 nm and a low-intensity positive band at ~540 nm (see Fig. 4a). This is in agreement with the coordination of the two carboxylate groups. In contrast with system I, the $|\Delta\varepsilon|$ values of the band at ~750 nm start to decrease at lower pH values (pH > 4.9), in parallel with the deprotonation of the [VOL^2] species. For a further increase of the pH in the range 7.5–12 the spectra remain roughly the same (Fig. 4b), corresponding to the formation of

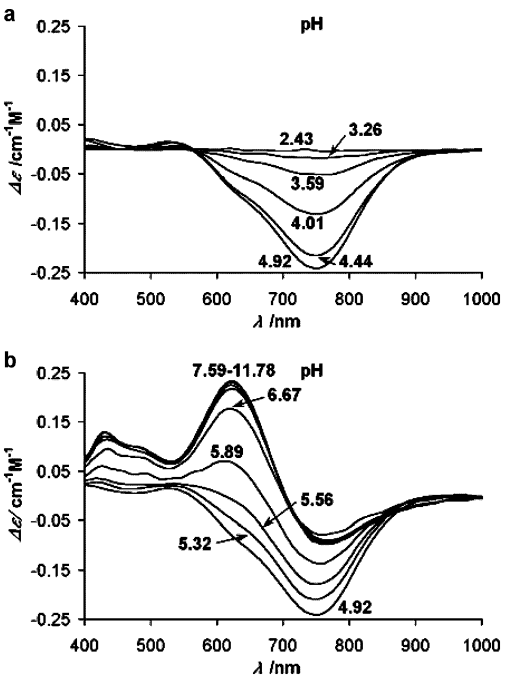

Fig. 4 CD spectra solutions containing $V^{IV}O^{2+}$ (0.003 mol dm^{-3}) and SalGly-L-Ala (0.004 mol dm^{-3}) at different pH values in the range: (a) 2.43–4.92 and (b) 4.92–11.78.

stoichiometry [VOL^{2}H$_{-2}$]$^{3-}$. In these spectra two main bands can be observed: at ~625 nm ($\Delta\varepsilon = 0.23$ mol^{-1} dm^{-3} cm^{-1}) and ~760 nm ($\Delta\varepsilon = -0.1$ mol^{-1} dm^{-3} cm^{-1}). Two other bands are seen at ~485 nm ($\Delta\varepsilon \sim 0.11$ mol^{-1} dm^{-3} cm^{-1}) and ~430 nm ($\Delta\varepsilon \sim 0.15$ mol^{-1} dm^{-3} cm^{-1}). These CD features of $V^{IV}O^{2+}$–SalGly-L-Asp are very similar with those of $V^{IV}O^{2+}$-SalGly-L-Ala,[8] which strongly suggests similar binding modes (*vide supra*) in the two systems, *i.e.* the carboxylate group of the Asp side-chain does not coordinate to $V^{IV}O^{2+}$.

Plausible binding modes

In order to elucidate the binding modes of the species, EPR spectra were measured both at room temperature and in frozen solution. The high-field region of the EPR spectra at 77 K, is depicted in Fig. 5 and 6. Table 2 includes the spin-Hamiltonian

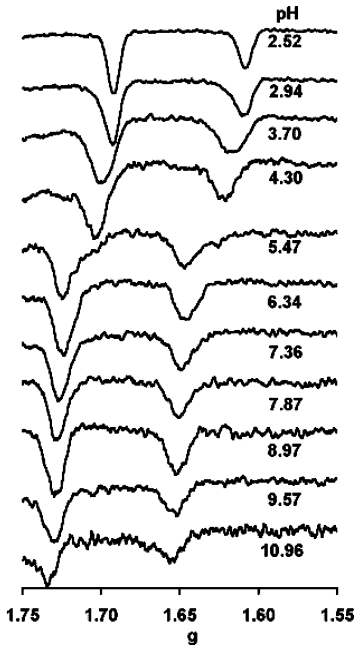

Fig. 5 High-field region of frozen solution EPR spectra (X-band) recorded at 77 K on the $V^{IV}O$-Sal-L-Asp system at a 1 : 2.6 metal ion to ligand ratio, at different pH values, $c_{VO} = 0.003$ mol dm^{-3}.

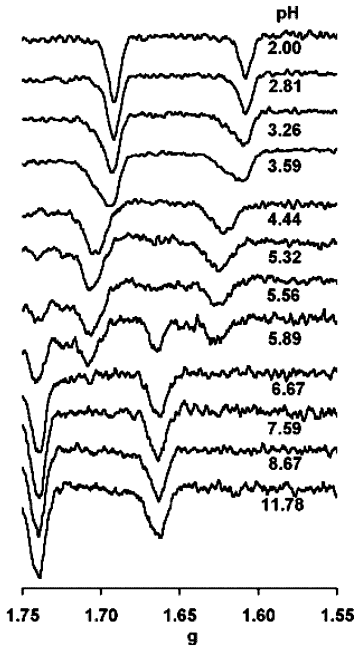

Fig. 6 High-field region of frozen solution EPR spectra (X-band) recorded at 77 K on the $V^{IV}O$-SalGly-L-Asp system at a 1 : 1.4 metal ion to ligand ratio at different pH values, $c_{VO} = 0.004$ mol dm^{-3}.

Table 2 Spin-Hamiltonian parameters ($g_{||}$ and $A_{||}$) obtained for the species formed in $V^{IV}O$–Sal-L-Asp and –SalGly-L-Asp systems. The EPR parameters were obtained by simulation of the spectra with the computer program of Rockenbauer and Korecz[12]

Species	Sal-L-Asp system			Proposed binding set
	$g_{||}$	$A_{||}$	$A_{||}^{est}$	
		$\times 10^4/cm^{-1}$		
$V^{IV}OL^1H_2$	1.935	177.9	177; 174	$(\alpha\text{-}COO^-, O_{amide}, 2 \times H_2O)_{eq}$; $(O^-, O_{amide}, 2 \times H_2O)_{eq}$
$V^{IV}OL^1H$	1.935	176.0	176; 170	$(2 \times COO^-, 2 \times H_2O)_{eq}$; $(\alpha\text{-}COO^-, O_{amide}, O^-, H_2O)_{eq}$
$V^{IV}OL^1$	1.938	174.0	170	$(O^-, O_{amide}, COO^-, H_2O)_{eq}(\beta\text{-}COO^-)_{ax}$
$V^{IV}OL^1H_{-1}$	1.947	165.2	165[a]	$(O^-, CON^-, COO^-, H_2O)_{eq}(\beta\text{-}COO^-)_{ax}$
$V^{IV}OL^1H_{-2}$	1.953	161.8	158[a]	$(O^-, CON^-, COO^-, HO^-)_{eq}$
$V^{IV}OL^2H_2$	1.935	178.0	177; 174	$(\alpha\text{-}COO^-, 2 \times O_{amide}, H_2O)_{eq}$; $(\alpha\text{-}COO^-, O_{amide}, 2 \times H_2O)_{eq}(O_{amide})_{ax}$
$V^{IV}OL^2H$	1.937	176.2	176; 170	$(2 \times COO^-, 2 \times H_2O)_{eq}$; $(O^-, O_{amide}, COO^-, H_2O)_{eq}(O_{amide})_{ax}$,
$V^{IV}OL^2$	1.939	173.3	166.8	$(O^-, O_{amide}, 2 \times COO^-)_{eq}(O_{amide})_{ax}$
$V^{IV}OL^2H_{-1}$	1.947	164	163[b]	$(O^-, CON^-, O_{amide}, COO^-)_{eq}$
$V^{IV}OL^2H_{-2}$	1.957	159.2	157[b]	$(O^-, 2 \times CON^-, COO^-)_{eq}$

[a] For CON^- contribution 38 was used. [b] For CON^-, a contribution of 36 was used (see text).

parameters obtained by simulation of the experimental spectra.[12] For the $V^{IV}O$ systems, Chasteen[13] introduced an additivity rule to estimate the hyperfine coupling constant $A_{||}^{est}$ ($A_{||}^{est} = \Sigma A_{||,i}$), based on the contributions $A_{||,i}$ of each of the four equatorial donor groups. The estimated accuracy of $A_{||}^{est}$ is $\pm 3\ 10^{-4}\ cm^{-1}$. Most of the $A_{||,i}$ were presented by Chasteen and values for the $A_{||}(CON^-)$ contributions were proposed by Cornman[14] and Costa Pessoa.[15] Following the suggestion of Tasiopoulos,[16] in this work we use different $A_{||}(CON^-)$ contributions in the range $36–40 \times 10^{-4}\ cm^{-1}$ depending on the total charge of the equatorial ligands.

We use $43.7 \times 10^{-4}\ cm^{-1}$ for the $A_{||}(O_{amide})$[17] and $42.1 \times 10^{-4}\ cm^{-1}$ for the $A_{||}(COO^-)$[18] contribution. These parameters can be used to predict the probable binding mode of each of the complexes formed, but care must be taken as the contributions of the donor groups to the hyperfine coupling constant may also depend also on their orientation,[19–20] or type of the axial ligand.[21] The influence of the axial donor groups (if any) is not taken into account.

The speciation curves (Fig. 1) indicate that complex formation starts at relatively low pH with the protonated species $[VOL^{1,2}H_2]^+$ and $[VOL^{1,2}H]$. In both systems, the EPR parameters and Vis spectra at low pH (*ca.* 2–3.3) indicate the presence of a mixture of $[VO(H_2O)_5]^{2+}$, $[VOL^{1,2}H_2]^+$ and $[VOL^{1,2}H]$ species. The binding mode of $[VOL^{1,2}H_2]^+$ possibly involves both the carboxylate (or the phenolate-O^-) and O_{amide} donors (see Scheme 2). The unambiguous appearance of the phenolate-O^- → $V^{IV}O$ CT band, in the Vis spectra of $[VOL^{1,2}H]$ indicates phenolate coordination, but probably Asp-type ($2 \times COO^-$ and 0, 1 or $2 \times O_{amide}$) coordination also occurs, and thus isomeric structures coexist in the solution. It is difficult to determine the exact EPR parameters for each of the species $VOL^{1,2}H_2$-$VOL^{1,2}H$-$VO^{1,2}L$, as the $A_{||}$ values change almost continuously in both systems in the pH range 3–5.5, and the individual spectra strongly overlap each other.

For both systems, the formation of $[VOL^{1,2}]^-$ gives rise to considerable changes in the CD spectra, due to the coordination of the Asp side-chain, and the maximum concentrations of the complexes corresponding to this stoichiometry are achieved at pH ~ 4.5 for system I, and ~5 for system II. Plausible binding modes are indicated in Scheme 2.

The next deprotonation step in both systems is ascribed to the amide deprotonation/coordination. For system I the $pK(VOL^1)$ value of 4.79 agrees with that for the corresponding complex $V^{IV}O$-SalGly (=4.76[3]), indicating close structural similarity between the complexes involved. The pattern of the CD spectra up to pH 6.3 remains approximately the same and is similar to that for $V^{IV}O^{2+}$–*N*-acetyl-L-aspartic acid system.[6] This suggests that the β-carboxylate of the Asp side-chain is in the coordination sphere and for steric reasons probably occupies the axial position in both $[VOL^1]^-$ and $[VOL^1H_{-1}]^{2-}$. This is also in agreement with the significantly higher $pK(VOL^1H_{-1})$ value of 8.09 as compared with that for $V^{IV}O$–SalGly (=7.57[3]) in which the axial position is occupied by an H_2O molecule. The proposed structure for the resulting species $[VOL^1H_{-2}]^{2-}$ is presented in Scheme 2.

For system II, the parallel deprotonation/coordination of the two amide groups are strongly cooperative processes, as was found for $V^{IV}O$–SalGly-L-Ala system.[4] The stepwise deprotonation constants of the two amide-NH groups are $pK(VOL^2) \sim 6.6$ and $pK(VOL^2H_{-1}) \sim 5.4$. Overall, the CD spectra differ from those of system I, indicating distinct coordination modes of the β-carboxylate group for the two ligands. The average p*K* of the processes determined by the different techniques (pH-metry: 6.12, Vis: 6.01, RT-EPR: 5.98, LN-EPR: 5.95, CD: 5.92) is approximately half a unit higher than that for the same processes in the system VO–SalGly-L-Ala. The presumed equatorial coordination of the carboxylate group of the Asp side-chain in $[VOL^2]^-$ is the cause of the difference: a structural rearrangement is necessary, in parallel with the deprotonation of the amide nitrogens. Species containing one deprotonated amide–N seem to be formed in negligible amounts, probably because the good anchoring donors present, a negatively charged phenolate–O^- on one side, and a negatively charged carboxylate–O^- on the other side, making the deprotonation/coordination strongly cooperative. Low temperature EPR measurements were made with nearly equimolar solutions in an effort to detect the monodeprotonated species $[VOL^2H_{-1}]^{2-}$. Samples with the same composition were measured both by CD and by EPR; some of the spectra are presented in Fig. 6. The EPR spectra show that the concentration of $[VOL^2]^-$ is approximately equal to that of $[VOL^2H_{-2}]^{3-}$ at around pH 5.8, and a low-intensity signal which can presumably be ascribed to $[VOL^2H_{-1}]^{2-}$ is also observed, its maximum relative concentration being ~10%. Accordingly, we can say that in system II there is high cooperativity in the deprotonation of the two NH_{amide} protons and the coordination of both CON^- donors (see also Table 2).

The room temperature EPR measurements (Fig. SI-2 in ESI†) also confirmed these findings: the spectra in the pH range 5–8 could be simulated within experimental error as a linear combination of the individual spectra of $[VOL^2]^-$ and $[VOL^2H_{-2}]^{3-}$. It is not necessary to presume formation of $[VOL^2H_{-1}]^{2-}$ to explain all the features of the room temperature EPR spectra. The CD measurements led to similar findings: (Fig. SI-3 in ESI†) it was possible to describe the system in the same pH range with two linearly independent CD spectra, those of $[VOL^2]^-$ and $[VOL^2H_{-2}]^{3-}$. This means again that complex $[VOL^2H_{-1}]^{2-}$ has almost no contribution to the CD. The

log β value of species $[VOL^2H_{-1}]^{2-}$ was estimated from the Vis (Fig. SI-4 in ESI†), and the LN EPR spectra (Fig. SI-5 ESI†). The spectral uncertainty of $[VOL^2H_{-1}]^{2-}$ species does not allow us to determine clearly which amide-NH deprotonates first, though, the missing CD intensity suggests the same sequence as in the case of the SalGly-L-Ala system, *i.e.* the amide-NH near the phenolate terminus deprotonates first, and the amide-NH near the carboxylate terminus second.

Conclusions

The speciation and solution spectral studies discussed above indicate that both the terminal COO^- and the phenolate-O^- can behave as anchoring donors to chelate the dipeptide and tripeptide-analogue ligands Sal-L-Asp and SalGly-L-Asp: both ligands are strong $V^{IV}O^{2+}$ binders and deprotonation of the amide-NH group(s) is induced by the metal ion in both systems.

A comparison of the two ligands indicates that presence of the β-carboxylate group has a different effect on the metal ion induced deprotonation and subsequent coordination of the peptide amide group. For the $V^{IV}O$–Sal-L-Asp system this takes place with a pK_a of 4.79, which is practically the same as that for SalGly (4.76).[3] However, further deprotonation (substitution of an H_2O ligand by OH^-) occurs with a significantly higher pK_a value (8.09), as compared with that of the corresponding $V^{IV}O$–SalGly complex (= 7.57[3]), in which the axial position is occupied only by a water molecule instead of a β-COO^- function.

As for SalGly-L-Ala, deprotonation of the two amide-NH groups of SalGly-L-Asp occurs in a cooperative way, but at a significantly higher pH; the pK_a values are 6.00 (5.37 for SalGly-L-Ala[4]), the difference being due to the effect of the equatorial coordination of the β-COO^- function of the Asp moiety. Coordination of the β-carboxylate of the Asp has also been observed to hinder amide-NH deprotonation in Cu(II) complexes.[22–25]

Acknowledgements

This work was carried out in the frame of a COST D21 project. The authors are grateful to the National Research Fund (OTKA T49417/2004), the Hungarian Academy of Sciences, the Fundo Europeu para o Desenvolvimento Regional, Fundação para a Ciência e Tecnologia, the POCTI Programme (project POCTI/QUI/56949/2000), the PhD grant SFRH/BD/6371/2001 and the Hungarian-Portuguese Intergovernmental S & T Co-operation Programme for 2004–2005.

References

1 I. Sóvágó, in *Biocoordination Chemistry*, ed. K. Burger, Ellis Horwood, New York, 1990, ch. 4, p. 134.
2 T. Kiss, T. Jakusch, J. Costa Pessoa and A. I. Tomaz, *Coord. Chem. Rev.*, 2003, **237**, 123.
3 T. Kiss, K. Petrohan, P. Buglyo, D. Sanna, G. Micera, J. Costa Pessoa and C. Madeira, *Inorg. Chem.*, 1998, **37**, 6389.
4 T. Jakusch, A. Dörnyei, I. Correia, L. Rodrigues, G. Tóth, J. Costa Pessoa, T. Kiss and S. Marcão, *Eur. J. Inorg. Chem.*, 2003, **11**, 2113.
5 A. Jancsó, T. Gajda, A. Szorcsik, T. Kiss, B. Henry, Gy. Vankó and P. Rubini, *J. Inorg. Biochem.*, 2001, **83**, 187.
6 J. Costa Pessoa, T. Gajda, R. D. Gillard, T. Kiss, S. M. Luz, J. J. G. Moura, I. Tomaz, J. P. Telo and I. Török, *J. Chem. Soc., Dalton Trans.*, 1998, 3587.
7 H. M. Irving, M. G. Miles and L. D. Pettit, *Anal. Chim. Acta*, 1967, **38**, 475.
8 L. Zékány and I. Nagypál, in *Computational Methods for the Determination of Stability Constants*, ed. D. Leggett, Plenum, New York, 1985, p. 291.
9 R. P. Henry, P. C. H. Mitchell and J. E. Prue, *J. Chem. Soc., Dalton. Trans.*, 1973, 1156.
10 A. Komura, M. Hayashi and H. Imagana, *Bull. Chem. Soc. Jpn.*, 1977, **50**, 2927.
11 L. F. Vilas Boas, J. Costa Pessoa, in *Comprehensive Coordination Chemistry*, ed. G. Wilkinson, R. D. Gillard and J. A. McCleverty, Pergamon Press, Oxford, 1987, vol. 3, p. 453.
12 A. Rockenbauer and L. Korecz, *Appl. Magn. Reson.*, 1996, **10**, 29.
13 N. D. Chasteen, in *Biological Magnetic Resonance*, ed. J. Lawrence, L. J. Berliner and J. Reuben, Plenum, New York, 1981, vol. 3, p. 53.
14 C. R. Cornman, E. P. Zovinka, Y. D. Boyajian, K. M. Geiser-Bush, P. D. Boyle and P. Singh, *Inorg. Chem.*, 1995, **34**, 4213.
15 J. Costa Pessoa, J. L. Antunes, L. F. Vilas Boas and R. D. Gillard, *Polyhedron*, 1992, **6**, 1449.
16 A. J. Tasiopoulos, A. N. Troganis, A. Evangelou, C. P. Raptopoulou, A. Terzis, Y. G. Deligiannakis and T. A. Kabanos, *Chem.-Eur. J.*, 1999, **5**, 910.
17 B. J. Hamstra, A. L. P. Houseman, G. J. Colpas, J. W. Kampf, R. LoBrutto, W. D. Frasch and V. L. Pecoraro, *Inorg, Chem.*, 1997, **36**, 4866.
18 T. Jakusch, P. Buglyó, A. I. Tomaz, J. Costa Pessoa and T. Kiss, *Inorg. Chim. Acta*, 2002, **339**, 119.
19 T. S. Smith, C. H. Root, J. W. Kampf, P. G. Rasmussen and V. L. Pecoraro, *J. Am. Chem. Soc.*, 2000, **122**, 767–775.
20 I. Cavaco, J. Costa Pessoa, M. T. Duarte, R. T. Henriques, P. M. Matias and R. D. Gillard, *J. Chem. Soc., Dalton. Trans.*, 1996, 1989.
21 J. T. Evangelos, K. D. Soulti, T. A. Kabanos, C. P. Themistoklis, C. P. Raptopoulou, A. Terzis and Y. Deligiannakis, *Chem. Commun.*, 2000, 601.
22 I. Sóvágó, T. Kiss and A. Gergely, *Inorg. Chim. Acta*, 1984, **93**, L53.
23 B. Decock-Le Reverend, A. Lebriki, D. Livera and L. D. Pettit, *Inorg. Chim. Acta*, 1986, **124**, L19.
24 I. Sóvágó, B. Radomska, I. Schn and O. Nyéki, *Polyhedron*, 1990, **9**, 825.
25 B. Decock-Le Reverend, L. Andrianariajona, C. Livera, L. D. Pettit, I. Steel and H. Kozlowski, *J. Chem. Soc., Dalton Trans.*, 1986, 2221.